Materials Research. 2018; 21(6): e20170244
DOI: http://dx.doi.org/10.1590/1980-5373-MR-2017-0244

Thermal Behavior of Pyrite in the CO_2 and N_2 Atmosphere for Obtaining Pyrrhotite: A Magnetic Material

***Eunice Machado de Oliveira*[a], *Camila Machado de Oliveira*[b]*, *Maria Virginia Bauer Sala*[c], *Oscar Rubem Klegues Montedo*[a], *Michael Peterson*[a,c]**

[a]*Programa de Pós-Graduação em Ciência e Engenharia de Materiais (PPGCEM), Universidade do Extremo Sul Catarinense, 88806-000, Criciúma, SC, Brasil*
[b]*Programa de Pós-Graduação em Ciência e Engenharia de Materiais (PGMAT), Universidade Federal de Santa Catarina, 88040-900, Florianópolis, SC, Brasil*
[c]*Departamento de Engenharia Química, Universidade do Extremo Sul Catarinense, 88806-000, Criciúma, SC, Brasil*

Received: March 02, 2017; Revised: July 19, 2018; Accepted: September 28, 2018

In the southern of Brazil the coal is composed of a large amount of pyrite (FeS_2), an environmental problem for this region because the pyrite turns a waste. This work investigated the behavior of pyrite in CO_2 and N_2 atmospheres, aiming to identify better thermal treatment conditions of the pyrite waste that favor obtaining a material with magnetic properties. The results show that the samples treated in both conditions presented hysteresis and some magnetic properties. The best results were obtained from N_2 because it is an inert gas, avoiding the pyrite oxidation and, consequently, favoring a major amount of pyrrhotite. The X-ray diffraction analyses showed that partial thermal decomposition of the pyrite occurs at 600 ºC. The total decomposition was reached at 800 ºC and the pyrrhotite phase was obtained. Such findings are relative new and can help enhance the utilization of pyrite, contributing to the environmental sustainability of the coal mining industry.

Keywords: *Pyrite, Pyrrhotite, Magnetic properties, Thermal treatment.*

1. Introduction

In the coal mining, after the extraction of ROM (Run-of-Mine / not classified ore) and the breaking of the largest blocks, the processing starts with the reduction of the ore sizes using an open crushing circuit and vibratory sieves, aiming a particle size near 1¼" (~ 3.2 cm). Following, the ROM is conduced to jigging. In this step, are obtained the processing coal (floated) and three sunken fractions: R1 - primary (rich in pyrite); R2 - secondary (rich in clays minerals) and R3 - tertiary (rich in carbon).

The processed coal is sieved in a 0.8 mm aperture sieve, resulting in a coarse product, which remains retained, destined to the thermoelectric. The passant is conduced to the fine concentration circuit, that include cyclones, tables and / or vibrating screens and flotation[1].

The Brazilian mineral coal has an elevated amount of impurities, 2% to 4% of sulphur and 40 to 60% of ashes, and the process is necessary to match the quality of products for thermoelectric plants. Thus, 60% of the ROM turns waste[2] and the fractions R1, R2 and R3 destined to the waste disposal cells[1].

This final destination causes one of the great problems related to the coal mining, the acid mine drainage (AMD), an effluent with elevate acidity levels which is a result from oxidation of the metal sulphides, such as pyrite, with the action of water and atmospheric air[3]. AMD contaminates the aquifers with bio accumulative heavy metals, making the water of the region improper for domestic and farming uses[4].

Studies show that the AMD can affect approximately 23000 km of water courses[5] and that the remediation for a typical abandoned mine needs the annual treatment of almost 3 million of cubic meters[6].

The disposal of wastes, besides AMD, also damage de landscape at the regions of coal mining, because the deposits need a large area[7].

Alternatives for the remediation of AMD are frequently studied[8-10]. However, the environmental problems can be avoided by the use of the mining wastes as raw material for other industrial activities[7]. The use of the fraction reach in pyrite and carbon would be reducing in 80 to 90% the potential of generation of acidity of the waste[11].

The decomposition reaction of pyrite varies according to the environment and the conditions in which they occur (atmosphere, temperature, particle size, flow conditions). These factors allow pyrite to transform into hematite, magnetite and/or pyrrhotite[12].

The phase changes promoted by thermal treatment of pyrite up to 800 ºC substantially increase its magnetization. These changes include the formation of magnetic phases such as pyrrhotite. In the thermal decomposition process, pyrite is transformed into pyrrhotite, and the FeS_2 grains become porous because of the loss of sulfur gas[13].

*e-mail: machadodeoliveirac@gmail.com

Materials with magnetic properties have magnetic moments that manifest very large and permanent magnetizations with the absence of an external field[14].

At ambient temperature, pyrite has paramagnetic properties, but when it is thermally treated and when the Curie temperature (Tc) is reached (between 280 and 320 ºC), pyrite is transformed into pyrrhotite, which can be ferromagnetic[15].

Technological devices are based on magnetism and magnetic materials, and there are major applications of materials with ferromagnetic properties. Examples of these applications include energy system distribution and generation, electromechanical conversion (cars and planes), electronics and telecommunication, transducers, sensing, medicine and biomedical engineering, computer science and industrial automation, among others[14].

In this context, the present work provides results regarding better reaction conditions for the coal mining waste composed of pyrite in N_2 and CO_2 atmospheres, aiming to obtain pyrrhotite with magnetic properties. This study can enhance the utilization of pyrite, contributing to the environmental sustainability of the coal mining industry.

2. Experimental

2.1 Materials

The pyrite used in this study was collected in Treviso, in Santa Catarina (Brazil). The material was passed through a milling process with a jaw crusher and a disk mill, and subsequently, an eccentric mill with alumina balls was used. The pyrite reached particle size after passing through a 60-mesh sieve.

2.2 Methods

2.2.1 Leaching

To reduce the amount of iron sulfates, the samples were leached in distilled water three consecutive times. Fifty grams of pyrite waste was immersed in 2 L of water at 80 ºC, and the system was subjected to magnetic agitation (Fitasom, model 752A, Brazil) for 20 min. The pyrite was separated by vacuum filtration (Prismatec, model 131, Brazil) and dried in a vacuum oven at 100 ºC for 24 h.

2.2.2 Thermal treatment

The thermal treatment of the leached pyrite was conducted in a horizontal and tubular kiln, and a refractory support was used to place the samples. The treatments were separately performed in CO_2 and N_2 atmospheres (White Martins). The temperatures and times of the treatments are shown in Table 1. The temperatures were chosen based on work Kopp and Kerr (1958), who evaluated by thermal analysis that the oxidation of pyrite begins at 538 ºC[16].

Table 1. Thermal treatment parameters.

Thermal treatment	Temperature (ºC)	Time (h)
A	Natural pyrite	
B	400	1
C	400	3
D	600	2
E	800	1
F	800	3

2.2.3 Characterization

2.2.3.1 X-ray diffraction - XRD

The crystalline phases present in the natural pyrite sample and in the samples subjected to the thermal treatments were identified with an XRD system (Shimadzu, Japan) equipped with a theta-theta goniometer and Cukα radiation at 1.5406 A. The step size used in the analysis was 2 º.min^{-1}. The measurement ranged between 10 and 80 º at 30 kV and 30 mA.

2.2.3.2 Infrared spectrometry (FTIR)

A FTIR spectrometer (Shimadzu, Japan) was used, and the analysis was performed by transmittance, with a 0.2 cm.s^{-1} speed and with a 4 cm^{-1} resolution ranging between 400 and 4000 cm^{-1}. For the analysis, the samples were pressed at an approximate proportion of 95% potassium bromide (KBr) and 5% sample.

2.2.3.3 Magnetometric analysis

The magnetic properties were evaluated with a Vibrating Sample Magnetometer - VSM (MicroSense, USA). The samples were subjected to an external magnetic field for the magnetic flux density measurement. The saturation magnetization values (Ms) and the remnant magnetization were defined in relation to the maximum value of the obtained field.

3. Results and Discussion

3.1 X-ray diffraction (XRD)

Figures 1 and 2 show the XRD results for the treated samples in the CO_2 and N_2 atmospheres, respectively. Both treatment samples are compared with the natural pyrite (A).

Figures 1 and 2 show the presence of one phase for the natural sample (A): pyrite (JCPDS: 42-1340). For the two evaluated atmospheres, the treatment performed at 400 ºC (B and C) did not promote a phase change of the material. Increasing the temperature to 600 ºC resulted in the partial decomposition of the pyrite, which refers to the pyrrhotite phase (JCPDS: 29-0724) identified by the X-ray patterns. The total decomposition of pyrite into pyrrhotite was observed at

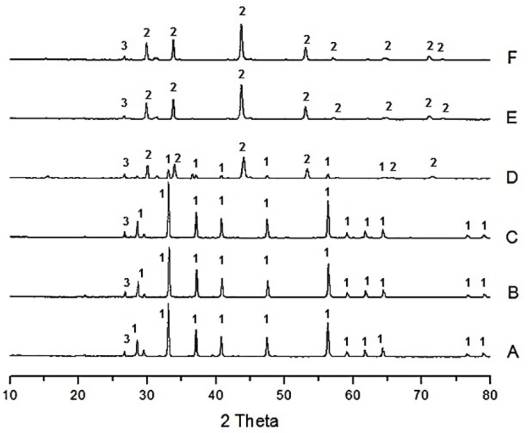

Figure 1. XRD of the samples treated in the CO_2 atmosphere: 1) pyrite; 2) pyrrhotite; 3) quartz.

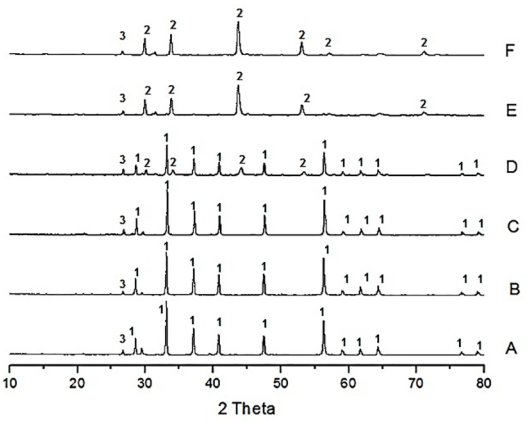

Figure 2. XRD of the samples treated in the N_2 atmosphere: 1) pyrite; 2) pyrrhotite; 3) quartz.

800 ºC (E and F). Quartz (JCPDS: 46-1045) was identified in all samples.

3.2 Infrared spectrometry (FTIR)

Figures 3 and 4 show the infrared spectra of the samples treated in the CO_2 and N_2 atmospheres, respectively, compared to the natural pyrite (A).

In Figure 3, peaks in the region around 422 cm^{-1} are characteristic of iron disulfide[17]. For the natural pyrite (A), there was a peak at 412 cm^{-1}, and for the samples treated in the CO_2 atmosphere, peaks at 416 cm^{-1} and 419 cm^{-1} were present at 400 ºC after 1 h (B) and 3 h (C), respectively.

For the pyrite at 600 ºC (D), which is partially decomposed, there was still a peak relative to iron disulfide at 419 cm^{-1}. For the samples treated at 800 ºC (E and F), the characteristic peaks of pyrite were not observed (total decomposition), and iron oxides peaks were present (433 cm^{-1})[18].

Peaks at 797 cm^{-1} and 800 cm^{-1} correspond to quartz[4]. The spectrum indicates the presence of iron sulfates in the samples, with bands near and between 900 and 1200 cm^{-1} [17].

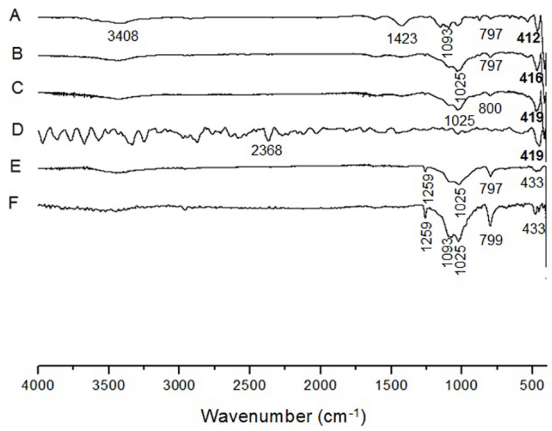

Figure 3. Infrared spectra of the samples treated in the CO_2 atmosphere.

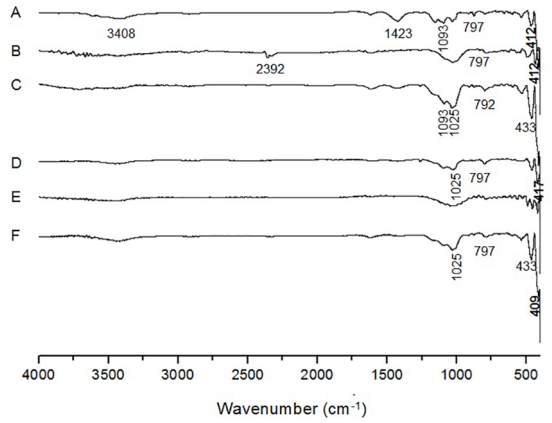

Figure 4. Infrared spectra of the samples treated in the N_2 atmosphere.

For the natural pyrite, there were absorption bands associated with the presence of carboxylic groups at approximately 1400 cm^{-1} (1423 cm^{-1} - Figure 3A)[19].

The peak identified in the natural pyrite around 3400 cm^{-1} is attributed to the presence of OH radicals groups[19].

The absorption regions of 2368 cm^{-1} (Figure 3D) and 2392 cm^{-1} (Figure 4B) corresponds to the presence of carbon dioxide[20].

For all samples, except for the sample treated at 400 ºC for 3 h (C) and for 800 ºC in 1 h (E), Figure 4 verifies peaks relative to iron disulfide (409 cm^{-1}, 412 cm^{-1}, and 417 cm^{-1})[17]. The samples that did not show that characteristic can be oxidized, as is the case of (C), for which the peak at 433 cm^{-1} corresponds to iron oxides[18].

The presence of peaks associated with FeS_2 at high temperatures suggests that the N_2 atmosphere is inert, while the CO_2 atmosphere is oxidant.

3.3 Magnetometric analysis

Figure 5 shows the obtained result for the natural pyrite.

Figure 5 does not show hysteresis, proving that the natural pyrite presents low magnetic activity.

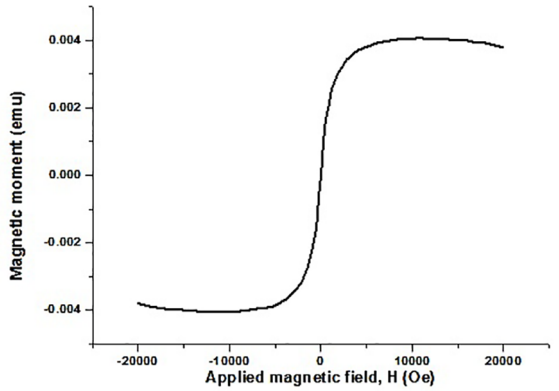

Figure 5. Magnetometric analysis of the natural pyrite.

The average saturation point, considering the increase and decrease of the applied magnetic field, was 4.06×10^{-3} emu (Ms). The average magnetization in the maximum applied field was 3.81×10^{-3} emu.

The figure shows a negative remanence (Mr) of -388.40×10^{-3} emu and a positive coercivity of 120007 Oe.

Figure 6 and Table 2 show the results of the samples treated in the CO_2 atmosphere.

Hysteresis was not verified in Figures 6B and 6C, proving that the treated samples at 400 ºC in the CO_2 atmosphere, for which the XRD analysis did not detect the presence of pyrrhotite, have low magnetic activity.

With increasing temperature, the partial and total decomposition of the pyrite (forming the ferromagnetic pyrrhotite phase; Figures 6D, 6E and 6F) and the presence of magnetic hysteresis cycle can be observed.

For the sample treated at 600 ºC for 2 h (Figure 6D), from saturation and based of the decrease of the H field by the reversion of the magnetic field direction, the curve did not return to its original shape at 0.48 Oe, producing the hysteresis effect (delay) in the magnetic moment relative to the H, decreasing to 0.07 Oe.

For the pyrite treated at 800 ºC for 1 h (Figure 6E), from saturation, the H field is reduced by the reversion of the magnetic field direction, and the curve did not return to its original shape at 0.14 Oe. At this point, there is a hysteresis effect in the magnetic moment relative to H, decreasing to 0.09 Oe.

For the sample treated at 800 ºC for 3 h (Figure 6F), from saturation, the H field is reduced by the reversion of the magnetic field direction, and the curve did not return to its original shape at 0.17 Oe, producing the hysteresis effect at the magnetic moment relative to H, decreasing to 0.05 Oe.

Figure 7 and Table 3 present the results of the samples treated in the N_2 atmosphere.

In the N_2 atmosphere, it can be observed that the realized treatments at 400 ºC (Figures 7B and 7C) also resulted in a material with low magnetic activity, and with increasing temperatures (Figures 7D, 7E and 7F), the presence of magnetic hysteresis cycle was verified.

For the sample treated at 600 ºC for 2 h (Figure 7D), from saturation, based on the decrease in the H field by the reversion of the magnetic field direction, the curve did not return to its original shape at 0.28 Oe, producing the hysteresis effect of the magnetic moment relative to H, decreasing to 0.003 Oe.

For the pyrite treated at 800 ºC for 1 h (Figure 7E), the measurement of the hysteresis showed the result of 0.39 Oe, which decreased to 0.00 Oe.

For the results of the sample treated at 800 ºC by 3 h (Figure 7F), the hysteresis was measured at 0.19 Oe, and it decreased to 0.08 Oe.

Comparing the XRD of the samples in the two atmospheres (Figures 1 and 2), it is observed that for D condition (600 ºC and 2 h) pyrrhotite peaks are more intense for CO_2, showing

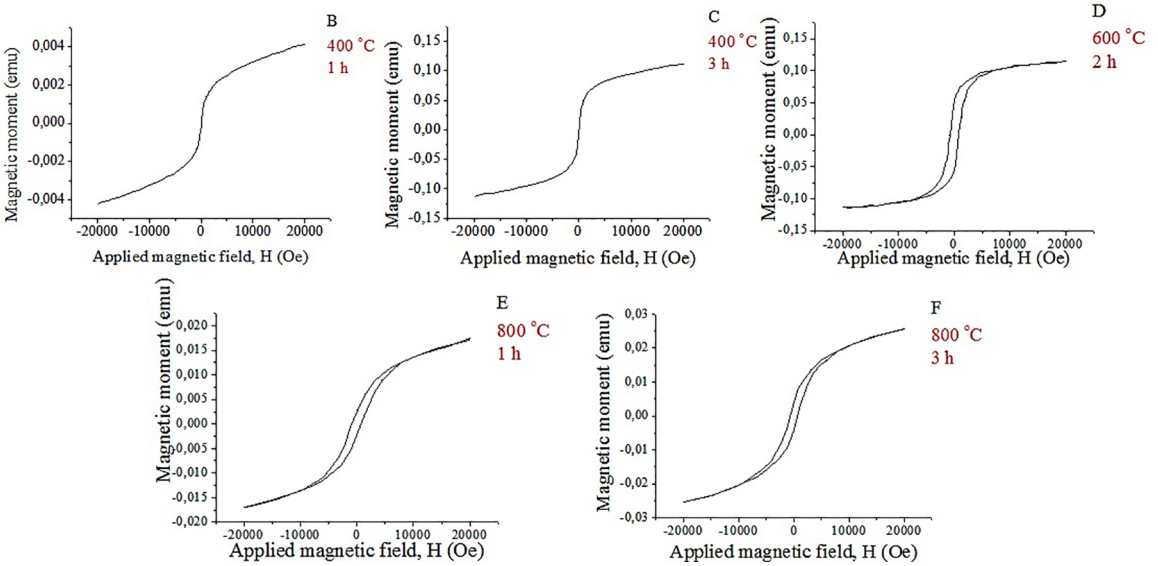

Figure 6. Magnetometric analysis of the samples treated in the CO_2 atmosphere.

Table 2. Magnetometric analysis results of the samples treated in the CO2 atmosphere.

Sample	M_s(× 10^{-3}emu)	Average magnetization of the maximum applied field (×10^{-3}emu)	Mr (× 10^{-3}emu)	Coercivity (Oe)
B	4.12	4.12	-196.66	64617
C	9.32	9.32	-889.23	84305
D	114.35	114.35	-54.85	799334
E	17.20	16.96	-2.56	840720
F	25.73	25.73	-4.37	691362

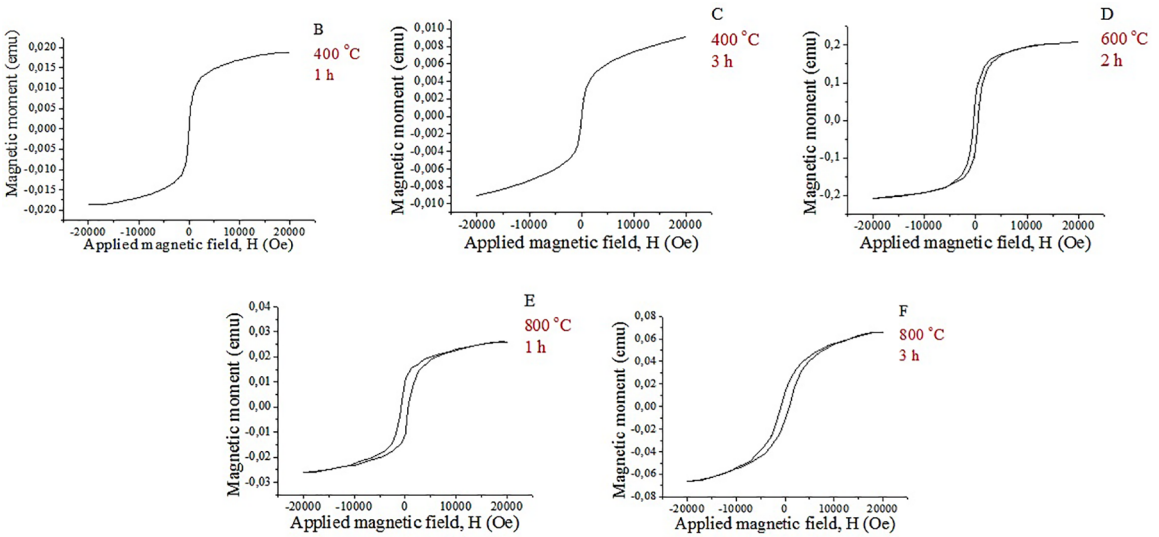

Figure 7. Magnetometric analysis of the samples treated in the N_2 atmosphere.

Table 3. Magnetometric analysis results of the samples treated in the N_2 atmosphere.

Sample	M_s(× 10^{-3}emu)	Average magnetization of the maximum applied field (×10^{-3}emu)	Mr (× 10^{-3}emu)	Coercivity (Oe)
B	18.84	18.64	-2.19	98698
C	9.08	9.08	-411.67	50312
D	208.94	208.89	-59.83	352955
E	26.14	26.01	-10.27	700975
F	66.10	65.96	-12.87	808948

that the decomposition of pyrite in this atmosphere is faster than in N_2. Lv et al. (2015)[21] indicated that this CO_2 effect is chemical in nature and is associated with the evolution of SO_2 and CO, according to Reaction 1[22]. Lv et al. (2015)[21] state that, although slower, the decomposition of pyrite under N_2 atmosphere results in a product with lower sulfur deficiency.

$$FeS_2 + 2CO_2 \rightarrow Fe_{1-x}S + 2CO + SO_2 \quad (1)$$

When the magnetometric analysis results are compared, for 800 ºC and for 3 h, the samples treated in both conditions presented hysteresis and some magnetic properties. Both conditions showed good results for obtaining a material with magnetic properties. The best results were obtained from N_2 because it is an inert gas, avoiding the pyrite oxidation and, consequently, favoring a major amount of pyrrhotite. Reaction 2 indicates the mechanism for the formation of iron oxide (Fe_3O_4) in CO_2 atmosphere[23].

$$3FeS_2 + 4CO_2 + 2CO \rightarrow Fe_3O_4 + 2COS \quad (2)$$

4. Conclusion

Aiming to identify better reaction conditions for pyrite waste from Santa Catarina in order to obtain magnetic properties, it was observed that:

1. The natural pyrite and the samples subjected to 400 ºC thermal treatment showed low magnetic activity;

2. Thermal treatments in both N_2 and CO_2 atmospheres at temperatures of 600 ºC and 800 ºC resulted in the formation of pyrrhotite. The samples treated in these conditions showed magnetic hysteresis cycle in the magnetometric analysis;
3. The pyrite decomposition into CO_2 is faster than in N_2. But the inert atmosphere avoids the iron oxides formation, and, consequently, ensures a greater amount of pyrrotitite.

The coal mining at southern Brazil, specifically in Santa Catarina State, contributed with the environmental problems of the region. Pyrite that is present in the waste of coal mining can be used for several industrial processes, including for the production of magnetic materials.

5. References

1. Soares PSM, Santos MDC, Possa MV, eds. *Carvão Brasileiro: Tecnologia e Meio Ambiente*. Rio de Janeiro: CETEM; 2008.
2. Nascimento FMF, Mendonça RMG, Macêdo MIF, Soares PSM. *Impactos ambientais nos recursos hídricos da exploração de carvão em Santa Catarina*. In: Congresso Brasileiro de Mina a Céu Aberto & II Congresso Brasileiro de Mina Subterrânea; 2002; Belo Horizonte, MG, Brazil.
3. Kontopoulos A. Acid Mine Drainage Control. In: Castro SH, Vergara F, Sánchez MA, eds. *Effluent Treatment in the Mining Industry*. Concepción: University of Concepción; 1998.
4. Evangelou VP. *Pyrite Oxidation and its Control*. Boca Raton: CRC Press; 1995.
5. Sasowsky ID, Foos A, Miller CM. Lithic controls on the removal of iron and remediation of acidic mine drainage. *Water Research*. 2000;34(10):2742-2746.
6. McKinnon W, Choung JW, Xu Z, Finch JA. Magnetic Seed in Ambient Temperature Ferrite Process Applied to Acid Mine Drainage Treatment. *Environmental Science & Technology*. 2000;34(12):2576-2581.
7. do Amaral Filho JR, Schneider IAH, de Brum IAS, Sampaio CH, Miltzarek G, Schneider C. Characterization of a coal tailing deposit for integrated mine waste management in the brazilian coal field of Santa Catarina. *Rem: Revista Escola de Minas*. 2013;66(3):347-353.
8. Campaner VP, Luiz-Silva W. Physical-chemical processes in acid mine drainage in coal mining, Southern Brazil. *Química Nova*. 2009;32(1):146-152.
9. Fungaro DA, Izidoro JC. Remediation of acid mine drainage using zeolites synthesized from coal fly ash. *Química Nova*. 2006;29(4):735-740.
10. Angioletto E, de Carvalho EFU, Biazini Filho FL, Lage Filho FA, Riella HG, Santos I, et al. *Ozônio na recuperação de solos e recursos hídricos contaminados por mineração*. Criciúma: UNESC; 2016.
11. Weiler J, do Amaral Filho JR, Schneider IAH. Coal waste processing to reduce costs related to acid mine drainage treatment - case study in the Carboniferous District of Santa Catarina State. *Engenharia Sanitária e Ambiental*. 2016;21(2):337-345.
12. Bhargava SK, Garg A, Subasinghe ND. In situ high-temperature phase transformation studies on pyrite. *Fuel*. 2009;88(6):988-993.
13. Waters KE, Rowson NA, Greenwood RW, Williams AJ. The effect of heat treatment on the magnetic properties of pyrite. *Minerals Engineering*. 2008;21(9):679-682.
14. Callister WD Jr., Rethwisch DG. *Materials Science and Engineering: An Introduction*. New York: Wiley; 2012.
15. Lowrie W. *Fundamentals of Geophysics*. Cambridge: Cambridge University Press; 2007.
16. Kopp OC, Kerr PF. Differential thermal analysis of pyrite and marcasite. *American Mineralogist*. 1958;43(11-12):1079-1097.
17. Dunn JG, Gong W, Shi D. A Fourier transform infrared study of the oxidation of pyrite. *Thermochimica Acta*. 1992;208:293-303.
18. Peterson M. *Produção de sulfato ferroso a partir da pirita: desenvolvimento sustentável*. [Thesis]. Florianópolis: Universidade Federal de Santa Catarina; 2008.
19. Landgraf MD, Alves MR, Silva SC, Rezende MOO. Caracterization of humic acids from vermicompost of cattle manure composting by 3 and 6 months. *Química Nova*. 1999;22(4):483-486.
20. NIST - National Institute of Standards and Technology. *Carbon dioxide*. Available from: <http://webbook.nist.gov/cgi/cbook.cgi?ID=C124389&Type=IR-SPEC&Index=1>. Access in: 20/11/2017.
21. Lv W, Yu D, Wu J, Zhang L, Xu M. The chemical role of CO_2 in pyrite thermal decomposition. *Proceedings of the Combustion Institute*. 2015;35(3):3637-3644.
22. Aylmore MG, Lincoln FJ. Mechanochemical milling-induced reactions between gases and sulfide minerals: II. Reactions of CO_2 with arsenopyrite, pyrrhotite and pyrite. *Journal of Alloys and Compounds*. 2001;314(1-2):103-113.
23. Aylmore MG, Lincoln FJ. Mechanochemical milling-induced reactions between gases and sulfide minerals: I. Reactions of SO2 with arsenopyrite, pyrrhotite and pyrite. *Journal of Alloys and Compounds*. 2000;309(1-2):61-74.